Earth Planet. Sci. Lett. xxx (xxxx) xxx

Contents lists available at ScienceDirect

Earth and Planetary Science Letters

journal homepage: www.elsevier.com/locate/epsl

Triple-oxygen isotopic evidence of prolonged direct bioleaching of pyrite with O_2

Issaku E. Kohl [a,*], Bryan Killingsworth [b], Karen Ziegler [c], Edward D. Young [d], Max L. Coleman [e]

[a] University of Utah, Department of Geology and Geophysics, Salt Lake City, UT 84112, USA
[b] United States Geological Survey, Geology, Energy & Minerals Science Center, 12201 Sunrise Valley Dr., Reston, VA 20192, USA
[c] University of New Mexico, Institute of Meteoritics, Earth and Planetary Sciences Department, 221 Yale Blvd NE, Albuquerque, NM 87131, USA
[d] University of California Los Angeles, Department of Earth Planetary and Space Sciences, 595 Charles E. Young Drive East, Los Angeles, CA 90095, USA
[e] NASA Jet Propulsion Laboratory, California Institute of Technology, 4800 Oak Grove Drive, Pasadena, CA 91109 and NASA Astrobiology Institute, Pasadena, CA 91109, USA

ARTICLE INFO

Edited by: Dr H Bao.

Keywords:
Triple-oxygen isotopes
Acidithiobacillus ferrooxidans
Sulfate
Pyrite oxidation
Geomicrobiology

ABSTRACT

Sulfate is often touted as containing atmospheric oxygen whose isotopic signature can constrain redox, environmental conditions, and biological activity. Yet, the amount and isotopic fractionation associated with air-O_2 incorporation during sulfate formation is still debated, making its verification difficult. In this study, we identify a distinct, microbially dominated environment with the potential to preserve maximum signals of air-O_2 in sulfate. We report triple-oxygen isotope data for sulfate produced from pyrite oxidation in microbial and abiotic experiments, and from natural dissolved sulfate from the Rio Tinto, Spain, an acid mine drainage site. The oxygen isotope systematics of sulfate in these environments define a unique kinetic isotope effect associated with initial stage pyrite oxidation by *Acidithiobacillus ferrooxidans* that preserves >80 % oxygen from air-O_2 in sulfate. Unlike experiments, which evolve toward water-oxygen dominated sulfate on short time scales, Rio Tinto, Spain hosts a microbe rich environment with distinct geochemistry that maintains high O_2-oxygen in sulfate. Therefore, in addition to containing isotopic records from water and air, sulfates can also contain a biosignature that is promising for understanding conditions on Mars and early Earth.

One Sentence Summary: Sulfate can contain > 80 % dissolved O_2-oxygen and triple-oxygen isotopes show kinetic effects associated with initial stage leaching by microbes.

1. Introduction

It is widely accepted that sulfate in the geologic record can contain remnants of atmospheric oxygen captured during oxidative sulfate production. Due to the non-labile nature of sulfate-oxygen, it is considered isotopically stable in rocks over geologic (billions of years) timescales (Chiba and Sakai, 1985; Rennie and Turchyn, 2014). This lack of isotopic exchange over long periods of time and some diagenetic conditions has allowed researchers to make transformative conclusions about the long-term and episodic evolution of Earth's atmosphere (Bao et al., 2008 and 2009; Crockford et al., 2016). Not only can sulfate act as a repository of atmospheric oxygen, but the oxidative weathering of reduced sulfur compounds acts as an oxygen sink, potentially buffering the early rise of atmospheric oxygen on Earth (Halevy et al., 2012). However, both above use cases are hampered by uncertainty in the assignment of the proportion of atmospheric oxygen in sulfate samples from both modern and ancient environments.

After isotopic signals of atmospheric O_2 were recognized in ancient sulfates originating from terrestrial pyrite oxidation (Bao et al., 2008), the origin of this signal was investigated in experiments (Kohl and Bao, 2011) and in modern rivers (Killingsworth et al., 2018; Hemingway et al., 2020). It has been more difficult, however, to make the link between sulfate's acquisition of oxygen from air-O_2 during pyrite oxidation on land to its preservation in marine sulfate eventually bound in rocks (e.g., Waldeck et al., 2019). For marine sulfate, the single largest reservoir, the amount of air-O_2 in sulfate is thought to be around 10 % due to competition between air-O_2 and Fe^{3+} during the oxidation of sulfate's precursor sulfite, which has experienced isotopic exchange

* Corresponding author.
E-mail address: issaku.kohl@utah.edu (I.E. Kohl).

https://doi.org/10.1016/j.epsl.2025.119639
Received 26 February 2025; Received in revised form 8 September 2025; Accepted 9 September 2025

with water (Cao and Bao, 2021 and references therein). The preferential study of marine sulfate is the result of its globally homogeneous isotopic composition and prevalence in the rock record, yet the muted air signals in marine sulfate may not be the best candidate when looking for remnants of past atmospheric oxygen (e.g., Waldeck et al., 2022).

If we consider early Earth, Mars, or other planetary environments where reservoir sizes, compositions, and dynamics could be significantly different from present-day Earth, it would be beneficial to identify extreme cases where the maximum atmospheric oxygen is preserved in sulfate. A wealth of data exists from natural systems and lab experiments, where reported atmospheric oxygen content in sulfate from sulfide mineral oxidation ranges from a 0 % to over 60 % (Taylor et al., 1984; Moses et al., 1987; Reedy et al., 1991; Descostes et al., 2004; Usher et al., 2004; Gleisner et al., 2006; Balci et al., 2007; Pisapia et al., 2007; Brunner et al., 2008; Hubbard et al., 2009; Tichomirowa and Junghans, 2009; Kohl and Bao, 2011; Heidel and Tichomirowa, 2011). However, it has proven difficult to relate evidence of high air-O_2 % and inferred mechanisms from lab-produced sulfate to observations from the field, which is the goal of the present study.

In oxic/aerobic environments where pyrite is oxidized in near surface environments, significant acid, sulfate, and iron accumulate in solution. Eventually these oxidation products can form iron sulfate minerals via pH changes and evaporative concentration. These iron oxyhydroxides and sulfates (e.g., goethite and hydronium jarosite), which have been identified on Mars, could contain clues concerning the conditions of their formation and the reaction mechanisms active in their production (Banfield et al., 2001; Fernandez-Remolar et al., 2004; Amils et al., 2007, 2014). The ubiquity of acidophilic, chemolithoautotrophic bacteria in contemporary terrestrial acid mine drainage (AMD) environments suggests such microorganisms could have played a role in the development and maintenance of such environments on early Earth and Mars (Yu et al., 2001; Fernandez-Remolar et al., 2004; Amils et al., 2007; Brunner et al., 2008; Hubbard et al., 2009).

To explore the role of microbes in determining the $\%O_2$ in pyrite-derived sulfate, we focus on pyrite oxidation in low pH conditions where microbes are known to catalyze the oxidation of pyrite-sulfur but the significance of the direct-O_2 pathway via atmospheric oxygen remains uncertain (Vera et al., 2022 and references therein). We use microbial laboratory experiments with *Acidithiobacillus ferrooxidans* and compare the environmental geochemistry and sulfate triple oxygen isotope systematics to sulfate from Rio Tinto, Spain, an AMD site and Mars analogue environment, where the same microbes are known to participate in weathering of pyrite-rich mine tailings (Amils et al., 2014).

2. Fundamentals and oxygen isotope geochemistry of pyrite oxidation

When sulfate is produced via oxidative weathering of sulfides, pH, pO_2, and [Fe^{3+}] work in concert to determine the O_2:H_2O ratio of the oxygen in the product sulfate (Singer and Stumm, 1970; Williamson and Rimstidt, 1994; Kohl and Bao, 2011). These distinct oxidation pathways are often represented by the overall reactions:

$$FeS_2 + 7/2O_2 + H_2O \rightarrow 2SO_4^{2-} + Fe^{2+} + 2H^+. \quad (1)$$

$$FeS_2 + 14Fe^{3+} + 8H_2O \rightarrow 15Fe^{2+} + 2SO_4^{2-} + 16H^+. \quad (2)$$

which are associated with 87.5 % air-oxygen (Eq. 1) and 0 % air-oxygen (Eq. 2). However, under most investigated conditions, the O_2:H_2O ratio in sulfate is assumed to be mediated by a balance between sulfite-water oxygen exchange and sulfite oxidation to sulfate, as SO_3^{2-} readily exchanges its oxygen with water and is the intermediate sulfoxyanion that precedes SO_4^{2-} (Betts and Voss, 1970; Horner and Connick, 2003; Brunner et al., 2005; Müller et al., 2013). Lower pH increases the sulfite oxidation rate, but it is thought that isotopic exchange outpaces sulfite oxidation by several orders of magnitude (Kohl and Bao, 2011; Müller et al., 2013). This has always been difficult to reconcile with experimental and natural data suggesting > 25 % air-oxygen is found in sulfate under certain conditions (Taylor et al., 1984; Pisapia et al., 2007; Tichomirowa and Junghans, 2009; Kohl and Bao, 2011; Killingsworth et al., 2022).

In both abiotic and microbially-mediated, low pH solutions, oxidation initially proceeds via reaction (1) where dissolved O_2 directly oxidizes pyrite sulfur, releasing sulfoxy anions and Fe^{2+}. $Fe^{2+}$is subsequently oxidized by O_2, forming Fe^{3+}, which accumulates in solution at low pH or precipitates at higher pH, eventually dominating the oxidation of pyrite sulfur due to the more favorable kinetic rate of reaction (2) (Williamson and Rimstidt, 1994; Brunner et al., 2008; Kohl and Bao, 2011). In the microbial case, this initial stage of oxidation via O_2, (Eq. 1) is associated with the lag phase of population growth (Brunner et al., 2008). Once Fe^{2+} accumulates in solution, the microbes begin to oxidize Fe^{2+} to Fe^{3+}, which occurs abiotically as well but at orders-of-magnitude slower rates, especially at pH below 2 (Rimstidt and Vaughan, 2014). This is referred to as the main stage of pyrite leaching where microbial production of Fe^{3+} facilitates indirect sulfide oxidation.

Despite these apparent environmental controls, $\delta^{18}O_{SO4}$ ($\delta^x O = (R^{x/16}_{smpl}/R^{x/16}_{std} - 1) * 1000$; where x refers to either ^{17}O or ^{18}O) reported for abiotic and microbially mediated oxidative sulfate production have significant overlap (Taylor et al., 1984; Moses et al., 1987; Reedy et al., 1991; Descostes et al., 2004; Usher et al., 2004; Druschel and Borda, 2006; Pisapia et al., 2007; Balci et al., 2007; Brunner et al., 2008; Hubbard et al., 2009; Tichomirowa and Junghans, 2009; Kohl and Bao, 2011). An exhaustive summary is presented by Gomes and Johnston (2017), which can be summarized as follows: 1) fractionation ($\varepsilon = 1000 \ln\alpha$) reported for $O_2 \rightarrow SO_4^{2-}$ is always negative and ranges from −3 to −25 ‰, with larger fractionations tending to be associated with microbial experiments, 2) fractionation for $H_2O \rightarrow SO_4^{2-}$ is highly variable in the literature and ranges from −8 to +20 ‰, and 3) all of these values are based on deconvoluting mixtures (Section 3, Eq. 3), where authors are forced to solve an equation with 3/5 of variables as unknowns. This highlights the ambiguity associated with determining % contribution from each oxygen source in sulfate without an independent tracer, which is crucial for the final determination of isotope fractionation factors. Despite these limitations, several studies have documented a clear time evolution in batch culture pyrite oxidation experiments where $\delta^{18}O_{SO4}$ evolves from early positive values, attributed to air-O_2 incorporation (Eq. 1) or sulfite-water oxygen exchange, to more negative values converging to within a few ‰ of $\delta^{18}O_{H2O}$ (Eq. 2) as experiments proceed (Taylor et al., 1984; Pisapia et al., 2007; Yu et al., 2001; Brunner et al., 2008; Tichomirowa and Junghans, 2009). In natural environments, higher $\delta^{18}O_{SO4}$ values have been associated with high flow rates of aerated waters in environments affected by AMD (Taylor and Wheeler 1994; Kim et al., 2019). These observations suggest that there may be cases of significant air-O_2 contributions to sulfate but this is untested by triple oxygen isotope techniques that could help quantify the contribution of O_2 and its controlling factors.

Currently, mid latitude terrestrial H_2O has a $\delta^{18}O$ of −20 to 0 ‰ with $\Delta^{17}O \approx 0$ to +0.04 ‰ ($\Delta^{17}O = \delta^{17}O - (\delta^{18}O * 0.528)$) and $\delta^{18}O$ of air-O_2 is 23.26 ‰ with a $\Delta^{17}O$ of −0.46 (Sharp et al., 2018; Young et al., 2014). Despite Bao et al. (2009) finding large-magnitude sulfate $\Delta^{17}O$ signals, which they attribute to atmospheric O_2 formed in very different pO_2:pCO_2 conditions to what we see today, there has been limited success in discriminating between water and air oxygen sources when sulfate $\delta^{18}O$ and $\Delta^{17}O$ variation is muted, such as in more recent environments (e.g., Hemingway et al., 2020; Killingsworth et al., 2022; Waldeck et al., 2022). It must also be considered that $\Delta^{17}O$ can change during utilization as mass fractionation lines associated with incorporation can and do diverge from the reference 0.528. Isotope effects attending the incorporation of air-oxygen into sulfate may result in a triple oxygen isotope slope whose net effect could mask any inheritance of negative $\Delta^{17}O$ from the air-O_2 oxygen source.

Additional complications are introduced by laser fluorination (LF), the main technique by which workers generate O_2 gas for triple oxygen isotopic measurements of sulfate. It has long been known that there are discrepancies between $\Delta^{17}O$ values generated in different labs, by different users, and different fluorination agents (F_2 vs BrF_5) (Bao and Thiemens, 2000a; Cowie and Johnston, 2016; Sharp and Wostbrock, 2021). Recently Wei et al. (2024) used a graphite reduction, CO high-voltage conversion to CO_2, CO_2-O_2 equilibration approach to generate 100 % yield, unfractionated O_2 from sulfate. Results suggest anywhere from 10–200 ‰ (0.01–0.2 ‰) positive artifacts in $\Delta^{17}O_{O2}$ are generated from the laser fluorination process, in addition to variable $\delta^{18}O$ fractionation, both resulting from fractionation associated with LF partial yields. Their study also suggests back-calculation of the original, unfractionated, $\Delta^{17}O_{SO4}$ based on partial yield LF data may be impossible because there is no theoretical basis for assigning a single, replicable, vector (triple oxygen fractionation slope) for the LF partial yield process. As the 10–200 ‰ (0.01–0.2 ‰) positive artifacts in $\Delta^{17}O_{O2}$ encompass roughly half the total measured range of terrestrial "mass dependent" $\Delta^{17}O$ values, these findings call into question the previous assumptions surrounding use of $\Delta^{17}O_{SO4}$ as an absolute tracer for oxygen sources.

In order to assess our ability to differentiate microbial from abiotic sulfate, determine significance of direct oxidation by O_2 and identify potential biosignatures, we ran a series of experiments oxidizing pyrite in sulfate-free, HCl media with and without *Af* and with and without $\Delta^{17}O$-labeled water, where the latter allows unambiguous tracing of oxygen sources and determination of the pyrite leaching stage (Fig. 1, Eq. 4). Then, with insights from the labelled experiments, the *Af*-mediated pyrite oxidation experiments with isotopically normal water characterize the "microbial end-member" in oxygen three-isotope space. Finally, constraints from the lab experiments are applied to oxygen isotope systematics of dissolved sulfate from Rio Tinto.

3. Methods and approach

$\delta^{18}O_{SO4}$ was measured at JPL on a Thermo Scientific MAT 253 IRMS with CO being produced via TC/EA. The average offset between TC/EA and LF measurements of our internal standard JPL-$BaSO_4$ (8.79 ‰ for Rio Tinto and 10.63 ‰ for experimental data, two different analysts) was applied to the $\delta^{18}O$ values measured from O_2 generated via LF for experimental and Rio Tinto sulfates. The $\Delta^{17}O$ of San Carlos Olivine (SCOL, the primary reference, which UCLA O_2 reference gas is calibrated to) is offset from VSMOW by −0.06 ‰ (Young et al., 2014; Pack et al., 2016; Sharp and Wostbrock, 2021). We use an additional −0.05 ‰ to account for Wei et al's (2024) LF correction for a total correction of −0.11 ‰, which is directly applied to the $\Delta'^{17}O$ (we use the logarithmic form for our data to linearize fractionation lines) values calculated from the measured O_2. We use a β of 0.528 for our reference frame.

Ultimately, any sulfate produced from oxidation of reduced sulfur species where air-O_2 and water are the oxygen sources has an isotopic composition defined by:

$$\delta^{18}O_{SO4}=m(\delta^{18}O_{H2O}+\varepsilon_{SO4\text{-}H2O})+(1\text{-}m)(\delta^{18}O_{O2}+\varepsilon_{SO4\text{-}O2}) \quad (3)$$

where the portion (m or 1-m) contributed from each source bears an isotopic composition of the source ($\delta^{18}O_{H2O}$ or $\delta^{18}O_{O2}$) adjusted for the isotopic fractionation attending the incorporation of that oxygen into sulfate (Van Stempvoort and Krouse, 1994). The use of $\Delta^{17}O$-labeled water eliminates the (ε) term from both sources in equation (3) resulting in the simplified equation:

$$\Delta^{17}O_{SO4} = m(\Delta^{17}O_{H2O}) \quad (4)$$

where (m) is the fraction of sulfate oxygen coming from water and $\Delta^{17}O$ is defined as:

$$\Delta^{17}O = \delta^{17}O - (\delta^{18}O^{*}0.528) \quad (5)$$

This is because $\Delta^{17}O$ is conserved during mass dependent isotope fractionation. If (m) and, by definition, (1-m) can be determined directly from $\Delta^{17}O$, then those values can be input back into equation (3) and ε's can be solved for empirically as long as >1 set of (m) values exist and the unknowns are reduced to 2 in 2 equations (SUP, Section 5).

Details of laboratory reactor experiment design, field sample collection, isotope measurement approaches, and all collected data are contained in the supplementary materials.

4. Results

4.1. Geochemistry of lab experiments

The series of pyrite oxidation batch reactor experiments yielded different sulfate production profiles depending on the presence or absence of *Af*. In the control reactors with no added *Af*, sulfate production was very slow and is characterized by an exponential function ($e^{0.0114x}$) and intercept of 19.4 ppm (SUP, Figure S1). This is considerably slower than the *Af* reactors, which show exponential curves between $e^{0.121}$ and $e^{0.137}$, a difference of approximately a factor of 10. Exponential regressions of all experimental data sets yielded intercepts between 18.88 and 19.39 ppm sulfate, suggesting that to be

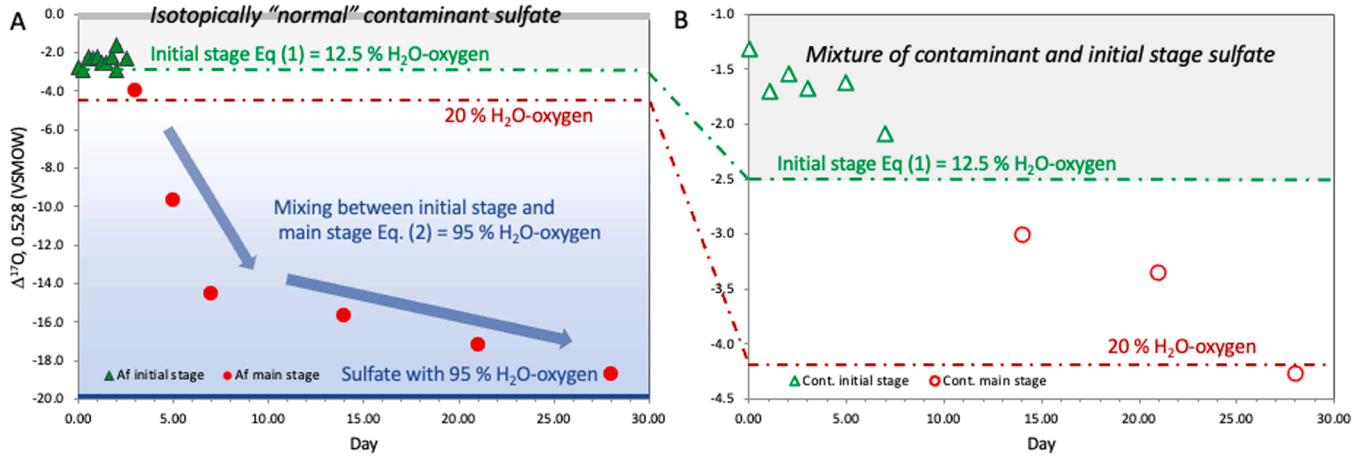

Fig. 1. A) Incorporation of isotopically labeled water in sulfate produced by Acidithiobacillus ferrooxidans (Af) with time. The initial stage of pyrite leaching, producing end-member Eq. (1) sulfate ($\Delta'^{17}O$ = −2.5 ‰), ends at approximately day 3 and sulfate production via Eq. (2) containing *ca.* 95 % water-oxygen incorporation begins. B) The control experiment without *Af* showed the same transition at day 10–11 (interpolated) but took 28 days to achieve the same $\Delta'^{17}O$ seen at day 3 in the *Af* experiment, suggesting a factor of 10 increase in overall oxidation rate resulted from microbial catalysis.

representative of the initial/contaminant sulfate pool (SUP, Figure S1). S/Fe starts sub-stoichiometric for all pyrite leaching experiments (stoichiometric = 2), yet for reactors containing *Af* it quickly evolves to greater than stoichiometric by day 3 (SUP, Figure S2). This is followed by a return to sub-stoichiometric by day 5 for the *Af* experiments, likely the result of decreasing pH and increasing Fe solubility. The control reactors show a steady S/Fe of 1.5 for the duration of the experiments.

4.2. Isotopically labeled lab experiments

Isotopically labeled water ($\Delta'^{17}O_{H2O} = -20$ ‰) constrains the transition from the initial (first 3 days for *Af*, 10–11 days for the control) to main stage pyrite leaching that we define using the stoichiometry of oxygen in pyrite-derived sulfate coming from the O_2 and Fe^{3+} (H_2O) pathways (Eqs. 1 and 2) in both experiments (Fig. 1, Table S2). The initial stage of the labeled water experiment containing *Af* produced sulfate with 8.75–15.15 % incorporation of isotopically labeled water-oxygen ($\Delta'^{17}O$ from −1.74 to −3.03 ‰), consistent with oxidation dominated by Eq. (1) (sulfate with 12.5 % water-oxygen is stoichiometric, Fig. 1A). After day 3 (end of initial-stage), the transition to sulfate production via Eq. (2) became apparent, characterized by incorporation of increasing amounts of labeled oxygen until day 28, when only 4.3 % air-O_2 remained in the accumulated sulfate (Fig. 1A). The final O_2:H_2O oxygen ratio was roughly 5:95, indicating stoichiometric oxidation by Eq. (2) overwhelmed the initial Eq. (1) sulfate.

In contrast to the *Af* experiment, $t = 1$ h sulfate from the abiotic control indicates 7 % of the sulfate-oxygen bears the isotopic label present in the water ($\Delta'^{17}O = -1.42$ ‰). Day 10–11 (interpolated) is when label incorporation in the abiotic control begins to match what we observed in the *Af* culture experiment after only 1 h (Fig. 1). There is evidence (abiotic reactors having a $\Delta'^{17}O < -2.5$ ‰) that a small amount of contaminant sulfate was present in the reactors after the addition of pyrite. We calculate this amount in 2 different ways yielding very different results (SUP, Section 4) and come to the conclusion that quantitative removal of this sulfate "blank" would be difficult and likely erroneous. It should also be noted that abiotic pyrite oxidation is ubiquitous and any differences between the *Af* and control experiments should be seen as the result of microbial activity.

4.3. Isotopically "normal" lab experiments

The transition timings from initial to main stage pyrite leaching were identified in the labeled experiments (section 5.2) with those timings applied to the isotopically normal microbial and abiotic experiments whose conditions were identical to the labelled experiments. We used the sulfate produced with water of natural abundance isotopic composition to evaluate the isotope effects associated with Eq. (1) and (2). $\delta'^{18}O$ values for all sub datasets were between 0 and −5 ‰, making it difficult to tease apart source ratios and isotope fractionation effects from this set of experiments. $\Delta'^{17}O$ values range from −0.081 to 0.013 ‰ for initial stage pyrite leaching and from −0.062 to 0.008 for main stage. Data from controls are similar to data from *Af* inoculated reactors except the main stage *Af* inoculated reactor sulfate, which shows more variation in both $\delta'^{18}O$ and $\Delta'^{17}O$ (Table S3).

4.4. Rio Tinto geochemistry

The Rio Tinto waters can be grouped into two main types, green waters and red waters, which are different in both color and chemistry (see supplementary video RTwaters.mp4). Green waters are characterized by extremely low pH between 0.9 and 1.2, very high SO_4^{2-} concentrations up to 1000 mM, high total Fe with 42–65 % as Fe^{2+}, and less than stoichiometric S/Fe ratios relative to pyrite (Fig. 3 and Table S2, SUP). These green waters are only found in association with direct drainage from outlets in the Copper Liquor Dam retaining wall, where waters are flushing through fine grained mine tailings (SUP, Figures S4 and S5). Red waters are characterized by pH between 2.25 and 3.25, SO_4^{2-} concentrations between 30 and 200 mM, much lower total Fe with only 1–20 % as Fe^{2+}, and S/Fe ratios from 2.2 to 98.8 (Fig. 2 and Table S2, SUP).

4.5. Rio Tinto sulfate-oxygen isotopes

The Copper Liquor Dam area and it's Fe^{2+} rich, green water contains sulfate with $\delta'^{18}O$ between 4.3 and 5.4 ‰ and $\Delta'^{17}O$ between 0.008 and −0.020. Samples obtained from Fe^{3+} rich red waters have lower $\delta'^{18}O$ (between 1.0 and −2.2 ‰), and higher $\Delta'^{17}O$ (between 0.082 and 0.010 ‰). A notable observation is a moderate positive correlation ($R^2 = 0.72$) between sulfate concentration and $\delta'^{18}O_{SO4}$, where high sulfate concentration green water has the most positive $\delta'^{18}O_{SO4}$, decreasing linearly to the most negative isotopic compositions being associated with lower sulfate concentrations (SUP, Table S2 and S3, Figure S7).

5. Discussion: geochemistry and isotope systematics

5.1. Geochemical features of "initial stage" vs "main stage" leaching

Initial stage leaching for our *Af* experiments, as defined in section 4.2, is confined to the first 3 days. This initial period where the oxidation of pyrite by O_2 dominates is associated with modest increases in sulfate and iron in solution and is thought to be associated with the progressive colonization of the pyrite surface by *Af* (Mielke et al., 2003). Sulfur/iron ratios are initially sub stoichiometric (S/Fe = 2 for pyrite) but rapidly evolve to super-stoichiometric, suggesting preferential liberation of sulfur from the pyrite surface. Unlike previous studies where initial stage leachate solutions remained sub-stoichiometric with respect to pyrite, our experiments show an initial increase to a maximum S/Fe of nearly 4 before dropping down to the characteristic 1.1 for the *Af* inoculated reactors (Descostes et al., 2004; Pisapia et al., 2007; Brunner et al., 2008). Abiotic reactors maintained a S/Fe ratio between 1.4 and 1.6 for the duration of the experiment (Figure S2, SUP). Such S/Fe ratios < 2 show the preferential release of Fe from pyrite that is typical of *Af* lag phase growth (Yu et al., 2001) but could also be the result of oxidation of FeS or CuS species, which consume acidity, or degassing of sulfur species (Brunner et al., 2008; Heidel et al., 2013).

Isotopically labeled water allows identification of initial stage pyrite oxidation by O_2 (Eq. 1), consistent with sulfate containing 87.5 % dissolved O_2-oxygen in the presence of *Af* (Stoichiometric Eq. 1, Fig. 1). The direct oxidation of pyrite sulfur by O_2 implies that Fe^{2+} concentrations are not yet high enough to make iron oxidation more metabolically favorable than sulfur oxidation, and that O_2 is still outcompeting Fe^{3+} when oxidizing sulfur. Therefore, waters associated with initial stage oxidation should favor Fe^{2+} over Fe^{3+}. In environments where microbes are facilitating oxidation, a low Fe^{3+} concentration could be considered evidence that microbial initial stage oxidation of pyrite-sulfur is active. A switch to microbial Fe^{2+} oxidation, that is normally energetically favored and rate limiting under abiotic conditions, would instead enhance Fe^{3+} concentrations. In contrast to the initial stage, main stage pyrite leaching is indeed associated with higher relative concentrations of Fe^{3+} as *Af* metabolism has shifted from oxidizing sulfur to oxidizing iron (Brunner et al., 2008). The microbially produced Fe^{3+} in turn becomes the main oxidant of sulfur, which produces sulfate with 100 % of its oxygen sourced from water via (Eq. 2). Therefore, we expect solutions associated with main stage leaching to have high relative Fe^{3+} concentrations, more negative $\delta^{18}O$ values, and close to stoichiometric S/Fe ratios. Super stoichiometric S/Fe have also been observed in previous studies and our experiments. However, in the case of Rio Tinto increases in S/Fe ratios in main branch red waters are attributed to precipitation of Fe-oxyhydroxides, mostly goethite, that is favored as pH increases above 2.5, conditions not observed in our or previous experimental reactors.

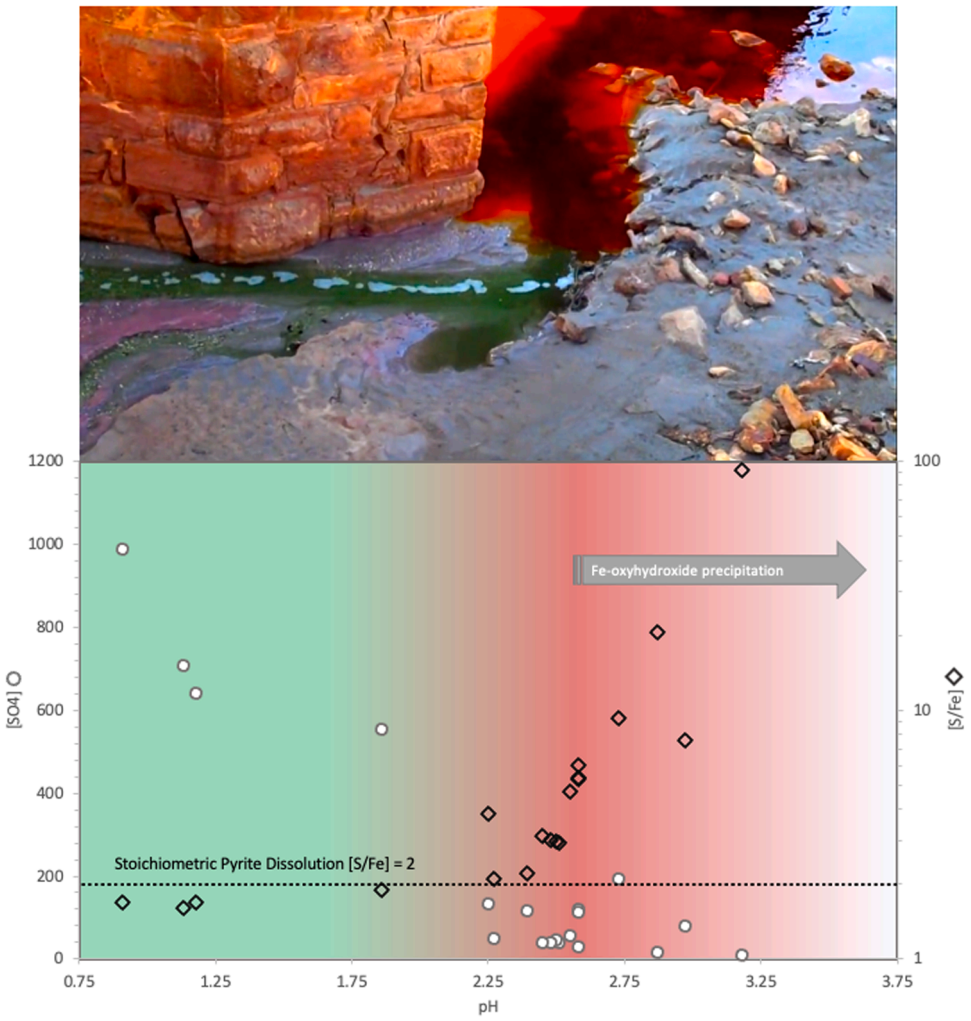

Fig. 2. Photo (screen shot from RTwaters.mp4) shows where samples 110116 and 110117 were collected. Saturation has been adjusted due to the angle of the sun causing the video to be very undersaturated. Green water is coming directly from Copper Liquor Dam through both subaerial and subsurface flow. The photo was taken where the green waters flow into the red waters of the Rio Tinto main branch. Sulfate concentration (white circles) and S/Fe ratio (black diamonds) vs. pH in Rio Tinto waters highlighting the presence of an end-member pH < 1 water containing slightly less than stoichiometric sulfate relative to iron (stoichiometric = 2 for pyrite dissolution). This S/Fe could result from the presence of sulfide minerals other than pyrite (e.g., FeS) but could also come from precipitation of efflorescent sulfate salts during evaporation. This end member water then evolves/mixes with higher pH waters of the main Rio Tinto branch resulting in rapid Fe-oxyhydroxide precipitation and S/Fe ratio rapidly increasing. The same green water data shows the maximum sulfate concentration at the outlet of Copper Liquor Dam, subsequent decreases are the result of dilution with some contribution from evaporative sulfate mineral precipitation.

5.2. *Isotope systematics of Rio Tinto sulfate: Fe^{2+} vs Fe^{3+} chemistry*

Using geochemical criteria previously defined in Section (6.1), we separated the sulfate data from the Copper Liquor Dam region green waters and that from the Rio Tinto main branch red waters. These distinct water types permit us to test the results of the microbial and control experiments and initial vs main stage geochemical criteria. We find that when using the leaching stage determination criteria defined in Section 5.1, the green, Fe^{2+} rich water from the Copper Liquor Dam region, which has high sulfate concentration with relatively high $\delta'^{18}O$ values, is likely associated with initial stage (Eq. 1) sulfate production.

The red waters display very different geochemistry and oxygen isotope systematics from the green waters (Figs. 2 and 3). Red waters Fe_{TOT} have 3–25 % Fe^{2+}, with 13 of 16 samples measuring below 10 % Fe^{2+}. This differs significantly from the green waters, which range from 42 – 65 % of Fe_{TOT} as Fe^{2+}. Oxygen isotope compositions of red water sulfate also imply a main stage leaching environment. $\delta^{18}O$ values are more negative (Fig. 3D) and suggest progressive mixing of (Eq. 2) derived sulfate into solutions initially dominated by (Eq. 1) sulfate from green water environments. This is supported by the environmental context of the different water chemistry niches. Copper Liquor Dam is an isolated tailings pile drainage, which eventually (between samples 110117 and 110116) mixes into the main branch red waters. The spatial evolution of sulfate oxygen isotopes in Rio Tinto is akin to the temporal evolution seen in the experiments (Fig. 3A and C).

5.3. *$\varepsilon^{18}O$ uses and limitations*

Previous studies have used $\delta^{18}O$ to apportion oxygen source ratios to sulfates produced from weathering of reduced sulfur minerals in the lab and in natural environments. This approach has yielded mixed results. The two oxygen sources have very different isotopic compositions (i.e. $\delta^{18}O$ of air-O_2 = 23.26 ‰ and $\delta^{18}O$ of waters, anywhere from 0 to −20 ‰ vs VSMOW). However, environmental sulfates from pyrite oxidation display a more muted range (−22 to 12 ‰ vs VSMOW; Killingsworth et al., 2022) indicating that there is likely a significantly negative $\varepsilon^{18}O_{SO4\text{-}O2}$ and/or most sulfate is dominated by water oxygen. $\varepsilon^{18}O_{SO4\text{-}H2O}$ appears to vary depending on pH, pO_2 and other geochemical conditions (Kohl and Bao, 2011) but can also appear to vary because of evaporation increasing the $\delta^{18}O_{H2O}$ as experiments

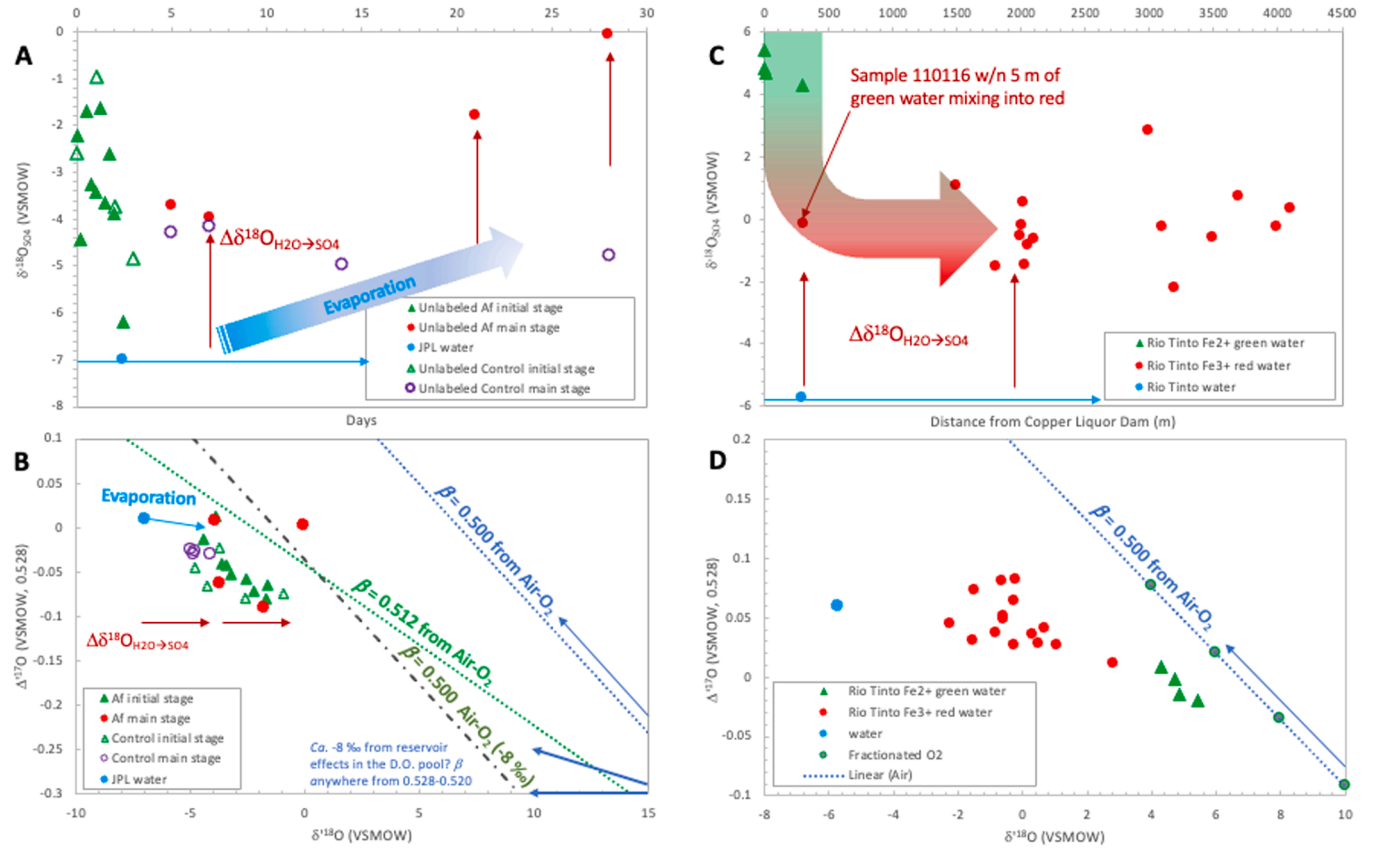

Fig. 3. A and C: $\delta'^{18}O$ vs time for sulfate from unlabeled pyrite oxidation reactors (A) and $\delta'^{18}O$ vs distance from the Copper Liquor Dam for Rio Tinto (C). For the *Af* inoculated reactor, approximately 5 ‰ of evaporation related fractionation can account for the increases in $\delta'^{18}O_{SO4}$ in the second half of the experiment, likely the result of not capping the flask properly. The control experiment (purple open circles) did not show this effect, with those sulfates having a constant main stage oxygen isotope composition. Rio Tinto data shows a similar initial decrease in $\delta'^{18}O_{SO4}$ followed by a leveling off despite maintaining a spread of roughly 5 ‰, which is likely the result of heterogeneous isolation and localized evaporation effects in the semi-arid Rio Tinto environment.
B and D: Triple-oxygen isotope compositions of sulfate from unlabeled experiments (B) and Rio Tinto (D). The relationship between Fe^{2+}-rich, green waters (green filled triangles) and Fe^{3+}-rich, main stage red waters (red filled circles) differs from the experiments to natural data in that both $\delta'^{18}O_{SO4}$ and $\Delta'^{17}O_{SO4}$ have significant overlap for the experiments while appear cleanly separated for Rio Tinto (likely an evaporation effect). Blue dotted lines represent a β of 0.500 extending from air O_2 at $\delta'^{18}O = 23.26$ and $\Delta'^{17}O = -0.463$. Another notable difference between the reactor experiments and Rio Tinto is the significantly more negative $\delta'^{18}O_{SO4}$ seen for the initial stage of the experiments. Error bars are the size of symbols or smaller.

proceed (Brunner et al., 2008). We have modeled potential ε pairs for O_2 and H_2O that satisfy the chemistry transitions observed in the labeled water oxidation experiments and reflect the % O_2 in sulfate that results from different oxidation pathways and mixtures of sulfate from both pathways as the experimental or natural conditions evolve (SUP, Section 5, Figure S8, Table S4).

The calculated $\varepsilon'^{18}O$ values are −17.3 ‰ and −2.3 ‰ for air and water, respectively, for Rio Tinto sulfate. However, these values cannot be used to interpret the experimental data, which gave −28.9 ‰ and +7.5 ‰ (*Af* unlabeled) and −29.9 ‰ and +12.0 ‰ (*Af* labeled) for respective $\varepsilon'^{18}O_{SO4\text{-}O2}$ and $\varepsilon'^{18}O_{SO4\text{-}H2O}$ pairs. The narrow range in $\delta'^{18}O$ (<5 ‰) observed for the unlabeled experiments make modeling and interpretation challenging. As shown (Figure 3A,C and S8), O_2 % does not clearly evolve with chemistry and experimental duration because % O_2 is directly dependent on $\delta'^{18}O_{H2O}$ in our model. This lack of relationship suggests that the fractionated oxygen from both sources has similar or changing $\delta'^{18}O$ values. This could be the result of a changing ε_{H2O}, evolving $\delta'^{18}O_{H2O}$, or a reservoir effect associated with rapid O_2 consumption. The above effects (or combination) do not manifest in the equivalent labeled water experiments due to the *ca.* +40 ‰ $\delta'^{18}O_{H2O}$, suggesting evaporation as the likely cause of the positive shift in sulfate oxygen isotopes with time in the unlabeled experiments. In Rio Tinto a positive correlation is observed for $\delta'^{18}O_{SO4}$ vs $[SO_4^{2-}]$, which suggests that more sulfate is being sourced from the green water than is being added as waters flow down the main branch (Figure S7). This helps to explain why the minimum $\%O_2$ calculated for Rio Tinto sulfate is *ca.* 40 % (Figure S8). In experiments this relationship is often reversed as sulfate accumulates with time and higher sulfate concentrations always occur at the end of experiments after much more sulfate has been produced via the Fe^{3+} pathway.

5.4. $\Delta'^{17}O$, $\alpha^{18}O$ and the role of β during oxygen incorporation

Brunner et al. (2008) was the first study to specifically highlight the significance of the role of *Af* in catalyzing pyrite oxidation during the initial leaching stage. However, they focus on the generation of sulfite and subsequent isotopic exchange with water and degassing of SO_2, which closes the sulfur isotope budget for their and other experimental studies (Yu et al., 2001; Descostes et al., 2004; Druschel and Borda, 2006). Given that the $\varepsilon'^{18}O$ value for sulfite-water oxygen exchange is between +10 and +15 ‰, this could explain sulfates with $\delta'^{18}O$ values in the 0–15 ‰ range (Brunner et al., 2005; Müller et al., 2013). Alternatively, sulfates with these high $\delta'^{18}O$ values could also be produced from oxidation by dissolved atmospheric oxygen, generating similar $\delta'^{18}O$ values if the $\varepsilon'^{18}O_{SO4\text{-}O2}$ value is between −10 and −25 ‰. Results from our isotopically labeled experiments provide clear evidence that sulfate oxygen is being sourced from dissolved O_2 during initial stage leaching. The isotopic fractionation associated with this direct oxidation

mechanism seen in Rio Tinto is determined to be −17.3 ‰ for $\varepsilon^{18}O_{SO4\text{-}O2}$, which is in a reasonable range to explain these and previous experimental data.

$\Delta'^{17}O$ on the other hand shows evidence for kinetic isotope fractionation. Accepting that initial stage sulfate-oxygen in the experimental reactors is sourced from dissolved O_2, we are forced to reconcile the $\Delta'^{17}O$ values observed in the natural abundance experimental reactors (Fig. 3). The corrected $\Delta'^{17}O$ data for these reactors are mostly slightly negative and range from 0.013 to −0.081 ‰ at $\delta'^{18}O$ values between −1.6 and −6.2 ‰. In order to achieve such a large change in $\Delta'^{17}O$ coupled to a roughly 25–30 ‰ change in $\delta'^{18}O$, requires that O_2 incorporation into sulfate follows a relatively shallow β. β values between 0.500 and 0.512 can reconcile the data considering the stoichiometry of (Eq. 1, Fig. 3B). This indicates that while initial stage oxidation of sulfur by O_2 (Eq. 1) dominates, the ^{17}O and ^{18}O relationships seen in nature are mixtures. While the possible range of 0.512- 0.500 is below the predicted lower limit for equilibrium β, it is possible that the true kinetic end member would, in fact, be 0.500 or less (Young et al., 2002; Bao et al., 2015; Hayles et al., 2017). The striking similarity of the triple-oxygen isotope systematics of sulfates from initial stage *Af* experiments and Rio Tinto green waters highlights sulfate-oxygen's potential as a biosignature. This scenario seems to demand further tests of whether similar environments to the Rio Tinto green waters could exist without microbes, or if microbial activity is required to sustain their sulfur and iron chemistry and the resulting shallow sulfate triple oxygen isotope slope. As it stands, the combination of well aerated, high flow waters with > 500 mM sulfate and > 50 % Fe^{2+} are difficult to reconcile with abiotic mechanisms.

6. Existing models

There is strong evidence in experimental and natural data for the direct involvement of air-O_2 in certain conditions, resulting in >25 % air-oxygen in sulfate (Taylor et al., 1984; Krouse et al., 1991; Pisapia et al., 2007; Heidel and Tichomirowa, 2011; This study). Despite this evidence, the electrochemical pyrite oxidation model of Rimstidt and Vaughan (2003), whereby sulfoxy-species are produced by step-wise nucleophilic attack of water on the sulfur site of pyrite remains the paradigm. Cao and Bao (2021) provide the most comprehensive synthesis of our current understanding of reaction mechanisms and associated isotope effects and only one scenario is presented where a maximum 25 % of oxygen in sulfate could come from O_2 during abiotic pyrite oxidation. Microbially assisted oxidation was suggested to always result in < 25 % oxygen from O_2. Thus, sulfates possessing ≤ 25 % O_2-oxygen would result from the branching ratio of SO_3^{2-} that has exchanged oxygen with water being oxidized by either Fe^{3+} or O_2 during the final oxidation step to sulfate. Such sulfate with ≤ 25 % O_2-oxygen is expected after the release of either SO_3^{2-} or $S_2O_3^{-}$ into solution from the sulfide mineral surface, with or without microbial catalysis, and across a broad range of pH. Because of relative rate differences where sulfite-water oxygen exchange outpaces sulfite oxidation by up to 10 orders of magnitude at pH 1 (Müller et al., 2013), for > 25 % O_2-oxygen in sulfate, mechanisms must exist where O_2-oxygen-bearing SO_3^{2-} or $S_2O_3^{-}$ are not available in solution for oxygen exchange prior to oxidation to sulfate.

Our labeled water experiments provide confirmation that despite some sulfate being present at the onset of experiments from this and other studies, the direct oxidation of sulfur by O_2 does occur, and under certain conditions, such as in the case of Rio Tinto green waters, the O_2 oxidation pathway can also be sustained. For example, pyrite-derived sulfate with large positive differences in $\delta^{18}O$ relative to ambient water have been observed in AMD, specifically associated with higher flow rates of aerated waters (Taylor and Wheeler, 1994). Such environments, e.g. Fe^{2+}-rich green waters flowing from Copper Liquor Dam in Rio Tinto, may favor oxidation by O_2 because Fe^{3+} does not accumulate in solution and low pH both favors Fe^{2+} and prevents precipitation of Fe^{3+} on the pyrite surface. Thus, "fresh" pyrite surfaces without Fe^{3+} oxyhydroxides can remain readily accessible to O_2. It is possible that other variables such as sulfide mineralogy and grain size, water table fluctuations, and O_2 saturation state also play a role in maintaining O_2 as the dominant oxidant but not enough is known to evaluate those variables at this time. Regardless of the exact environmental controls, which must be evaluated in future studies, these data indicate that it is possible to maintain the environmental conditions necessary for a pyrite weathering regime where air-O_2 dominates the oxygen pool of the sulfate products.

7. The role of microbes

Explaining >25 % air-O_2 contribution to pyrite-derived sulfate is challenging for existing models and proposed reaction networks. While sulfate with >25 % air-O_2 is observed in our experiments and prior studies (e.g., Tichomirowa and Junghans, 2009), such high-O_2 sulfate is normally a transient feature. Our results from Rio Tinto show spatially and chemically distinct waters hosting sulfate with >80 % and 40–70 % from O_2. Such perpetually maintained oxygen contents in pyrite-derived sulfate in Rio Tinto may require microbial involvement and specific environmental conditions. Here we consider the role of microbes in maintaining >25 % air-oxygen in sulfate in Rio Tinto by proposing a pyrite oxidation pathway that could achieve such high O_2 contents, as existing models are inadequate.

There are no proposed reaction mechanisms that allow for sulf-oxy species other than S^0(rarely), thiosulfate, sulfite and sulfate (rarely) to be released into solution from the pyrite surface. The proposed mechanism that could directly release sulfate into solution from pyrite relies on nucleophilic attack of water, producing sulfate with 100 % water-oxygen (Eq. 2). Further, for >25 % O_2-oxygen in sulfate, sulfite-water oxygen exchange is not viable. Alternatively, intracellular enzymatically catalyzed sulfur redox transformations could explain the extreme O_2 content and associated isotope effects found in Rio Tinto green water sulfates. Unlike abiotic pathways, microbially catalyzed oxidation pathways contain several branching points where reduced sulfur can be transformed into sulfate without transitioning through SO_3^{2-}, thus avoiding oxygen exchange with water and preserving the source oxygen involved in the initial oxidation steps. Similar pathways have been proposed for abiotic sulfate production (e.g., Druschel and Borda, 2006) but have been largely discounted due to lack of conclusive determinations of high proportions of O_2-oxygen in abiotically produced sulfate. The initial sulfur species released from the mineral surface is dependent on mineralogy (In general, H_2S for acid soluble sulfides vs thiosulfate for acid insoluble sulfides), where heterogeneous mineralogy is the norm in natural systems (Bao et al., 2022). After $S_2O_3^{2-}$ forms inside or is transported to the periplasm it experiences enzymatic oxidation to tetrathionate ($S_4O_6^{2-}$) (Vera et al., 2022; Jones and Santini, 2023 and references therein). The $S_4O_6^{2-}$ is then disproportionated, facilitated by the enzyme tetrathionate hydrolase (TetH), forming elemental sulfur (S^0), $S_2O_3^{2-}$, and SO_4^{2-}. In most bioleaching models the active oxidant involved in these reactions is Fe^{3+} but in high flow, extremely acidic (pH <1.5), aerated environments our results suggest that the oxidation potential of dissolved O_2 is much greater than Fe^{3+}.

The thiosulfate pathway facilitates recycling, whereby S^0 is oxidized to $S_2O_3^{2-}$, then oxidized to $S_4O_6^{2-}$ by the enzymes thiosulfate-quinone oxidoreductase (TQO) and/or thiosulfate dehydrogenase (TSD), followed by TetH mediated disproportionation (Fig. 4). Disproportionation again produces S^0, which then begins the oxidation process anew, with respect to oxygen addition onto sulfur. Here, we have a mechanism for incorporating O_2 into SO_4^{2-} without involving an SO_3^{2-} intermediate and therefore much less potential for isotopic exchange with water on the way to forming SO_4^{2-}. This direct oxidation pathway and associated reaction network is therefore capable of producing sulfate with 80 - 90 % air-O_2 oxygen as long as dissolved oxygen activity remains high in the periplasm and cytoplasm of the aerobic sulfide oxidizing microbes, in

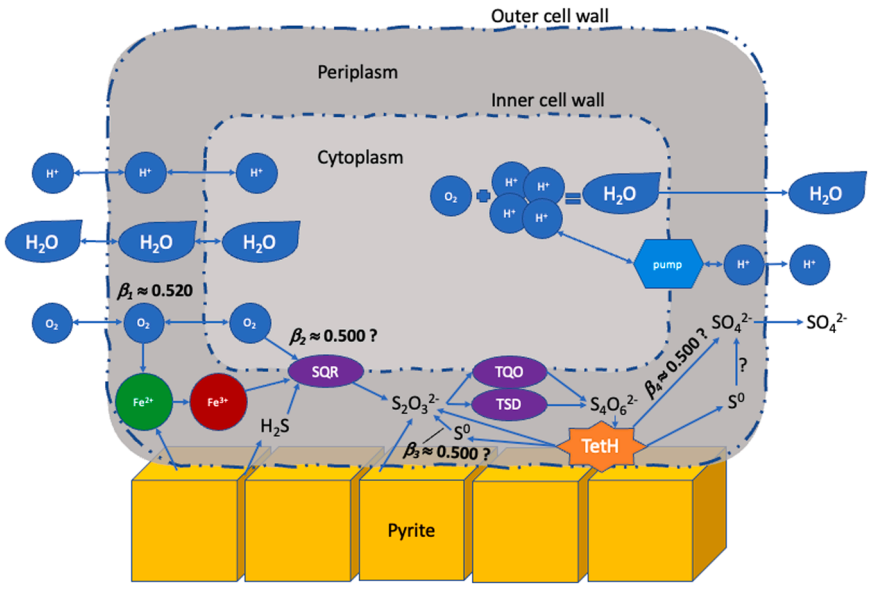

Fig. 4. Schematic view of the intracellular reaction network for pyrite oxidation by Acidithiobacillus ferrooxidans (Af). In general, for the direct oxidation mechanism to operate, cells need to be in direct contact with the mineral surface. $S_2O_3^{2-}$ is produced either on the mineral surface or from pumping in of liberated H_2S via the SQR enzyme, which can utilize either Fe^{3+} or O_2 as oxidants. Thiosulfate is then further oxidized to $S_4O_6^{2-}$ by either TQO or TSD in the periplasm. This is followed by disproportionation of $S_4O_6^{2-}$ to SO_4^{2-}, S^0, and $S_2O_3^{2-}$, facilitated by TetH. The fate of the resulting S^0 is uncertain and pathways exist for the stepwise oxidation to either SO_4^{2-} or $S_2O_3^{2-}$. The S^0 to SO_4^{2-} pathway is either dominated by O_2 as the oxidant or contributes a small amount to the overall SO_4^{2-} production if oxidized by Fe^{3+}. The most likely scenario explaining the *ca.* 90 % air-O_2 in initial *Af*-produced experimental SO_4^{2-} and Rio Tinto green water SO_4^{2-} is that $S_2O_3^{2-}$ in the periplasm already bares a dominantly air-O_2 signal via SQR mediated oxidation (β_2). This would then be inherited by $S_4O_6^{2-}$, and subsequently disproportionated SO_4^{2-}. It is also feasible that S^0 from disproportionation is oxidized to $S_2O_3^{2-}$ with O_2 and that either β_3 or β_4 is the source of the extreme β observed in these data.

this case, *Af*. Also shown (Fig. 4) are proton pump(s), which facilitate the formation of water from dissolved O_2 and free protons. The role of this mechanism and the potential for interaction between this *in-situ* produced water, bearing oxygen from dissolved O_2 is not clear but has the potential to result in indirect incorporation of O_2-oxygen into sulfate. Krouse et al. (1991) documented oxygen exchange between isotopically labeled O_2 and water during microbial pyrite oxidation experiments, likely resulting from this intracellular water production mechanism. However, the amount of air-O_2-water exchange needed to generate an appreciable change in the natural abundance isotopic composition of ambient water is unrealistically large given the constant exchange between cellular and ambient water.

8. A new model for O_2 incorporation followed by mixing

To evaluate the role of kinetic mass dependent fractionation between

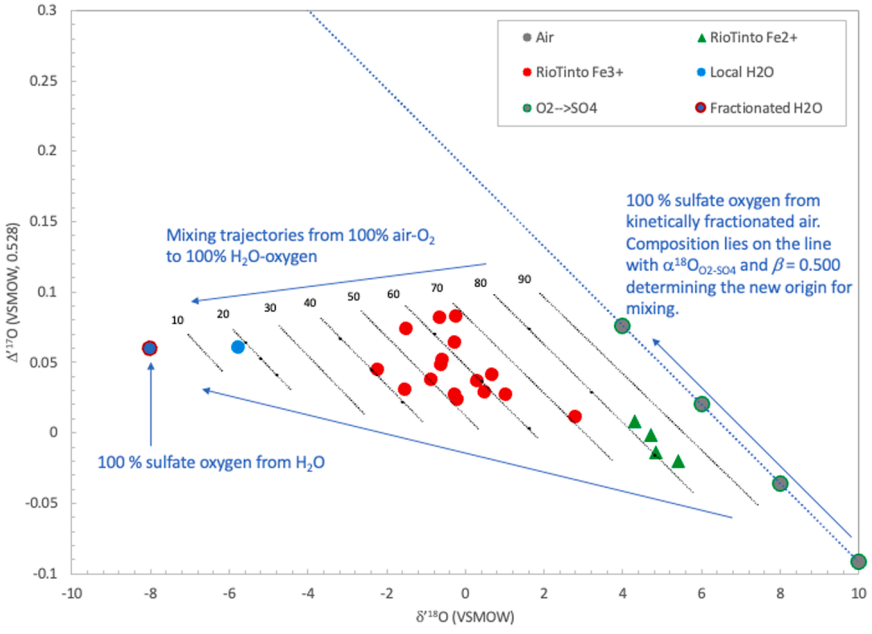

Fig. 5. Final mixing model showing Rio Tinto (green triangles) kinetically fractionated, initial stage sulfate with most of its oxygen coming from air, and the mixtures with main stage sulfate containing more water oxygen (red circles). The spread in $\Delta'^{17}O$ values for the red water sulfates may result from variable amounts of evaporation in ponds and tributaries within localized microenvironments.

air-O_2 and sulfate during initial stage *Af* pyrite oxidation we draw on the conclusions put forth by Angert et al. (2003) and Helman et al. (2005). Both studies show photorespiration associated with carbon fixation results in a β_{eff} (lambda) of 0.506 ± 0.005. A β of 0.521 is also reported for diffusion, which is too high to explain the measurements associated with the *Af*-produced, initial stage sulfate, but could be the source of the −8 ‰ $\delta'^{18}O$ offset observed in the lab experiments (Fig. 3B).

This evidence of enzymatically catalyzed O_2 utilization in oxidative reactions resulting in low β_{eff} values supports our conclusion that a similar mechanism is operative during the initial stage of pyrite leaching by *Af*. We propose a simple kinetic model whereby the initial stage, *Af*-catalyzed, direct oxidation of sulfur incorporates oxygen into sulfate with a β of 0.500 (Figs. 3 and 5). This is a multistep process with the initial step being the cellular uptake of O_2 from the dissolved O_2 reservoir. Like the photorespiration example, diffusion or pumping in of O_2 from the environment is unlikely to be associated with an extreme β. Subsequent steps attending enzymatic utilization of this O_2 are better candidates for reactions expressing more extreme KIE, which could also result in variable amounts of fractionation in triple-oxygen isotope space (i.e. resulting in different "end-member" compositions on the 0.500 line with air-O_2 as the origin, Fig. 3D). When considering the source of the extreme β_{eff} observed for the initial stage *Af* experiments and the Rio Tinto green waters, we favor the polythionate disproportionation reaction (β_4) as this represents a unidirectional, destructive reaction that directly yields sulfate. However, KIEs could also be associated with the production of thiosulfate via SQR (β_2) or the direct oxidation of S^0 by O_2.

During the transition from oxidation via O_2 (Eq. 1) to Fe^{3+} (Eq. 2), the initial stage O_2-bearing sulfate begins to mix with sulfate from Fe^{3+}-catalyzed oxidation with 100 % H_2O-oxygen. In $\delta'^{18}O$ space, the isotopic composition of this main stage sulfate is the result of the local water $\delta'^{18}O$ adjusted for the $\varepsilon_{H2O\text{-}SO4}$ (Fig. 5). For the labeled water experiments and the Rio Tinto sulfate, a 2-end-member mixing scenario best explains the data and evolving $\%O_2$ in sulfate (SUP, Figure S7 and Table S4).

9. Conclusions

Comparisons of sulfate triple-oxygen isotopic signatures from lab experiments and field samples from Rio Tinto of microbial and abiotic, pyrite-derived sulfate demonstrate 1) there are clear geochemical indicators distinguishing initial stage from main stage sulfate, 2) the rate attending initial stage microbial pyrite oxidation can be *ca.* 10x faster than abiotic pyrite oxidation, 3) the proportion of oxygen in pyrite-derived sulfate from O_2 is *ca.* 90 % at maximum and 4) there are environments on modern Earth where the O_2 (Eq. 1) pathway dominates and evolution toward a water-oxygen dominated system does not appear to be occurring. These findings suggest that the specific environments with the highest possible amount of atmospheric-O_2 in sulfate could be preserved in the geologic record and could be identified using geochemical indicators like iron speciation and paleo-environmental facies.

CRediT authorship contribution statement

Issaku E. Kohl: Writing – review & editing, Writing – original draft, Methodology, Investigation, Formal analysis, Data curation, Conceptualization. **Bryan Killingsworth:** Writing – review & editing, Writing – original draft, Formal analysis, Data curation. **Karen Ziegler:** Investigation, Formal analysis, Data curation. **Edward D. Young:** Supervision, Conceptualization. **Max L. Coleman:** Writing – review & editing, Supervision, Resources, Methodology, Funding acquisition, Data curation, Conceptualization.

Declaration of competing interest

The authors declare that they have no known competing financial interests or personal relationships that could have appeared to influence the work reported in this paper.

Acknowledgements

Supported by NASA Astrobiology Institute awards, # 05-NAI05-08 and # 12-NAI6-0005 to MC via the Wisconsin Astrobiology Research Consortium. We thank Dan McCleese for his support of part of the work via JPL RTD award to MC, # R.07.023.011. BK acknowledges support of the USGS. Mineral Resources Program. We thank Maite López of the Fundación Río Tinto for approval to sample in Rio Tinto and help over a number of years' field work. Part of the work was carried out at the Jet Propulsion Laboratory (JPL), California Institute of Technology, under contract with the National Aeronautics and Space Administration (80NM0018D0004). We thank Justin Christensen for his assistance in performing analyses, while holding a Caltech Summer Undergraduate Research Fellowship at JPL, and Randall Mielke for his assistance in performing the experiments. Any use of trade, firm, or product names is for descriptive purposes only and does not imply endorsement by the U. S. Government.

Supplementary materials

Supplementary material associated with this article can be found, in the online version, at doi:10.1016/j.epsl.2025.119639.

Data availability

Raw data will be made available on request.

References

Amils, R., Gonzales-Toril, E., Fernandez-Remolar, D., Gomez, F., Aguilera, A., Rodriguez, N., Malki, M., Garcia-Moyano, A., Fairen, A.G., de la Fuente, V., Sans, J. L., 2007. Extreme environments as Mars terrestrial analogues: the Rio Tinto case. Planet. Space Sci. 55, 370.

Amils, R., Fernandez-Remolar, D., Team, the IPBSL, 2014. Rio Tinto: a geological and mineralogical terrestrial analogue of Mars. Life 4, 511–534.

Angert, A., Rachmilevitch, S., Barkan, E., Luz, B., 2003. Effects of photorespiration, the cytochrome pathway and the alternative pathway on the triple isotopic composition of atmospheric O2. Global Biogeochem. Cycles (17), 1030.

Balci, N., Shanks III, W.C., Mayer, B., Mandernack, K.W., 2007. Oxygen and sulfur isotope systematics of sulfate produced by bacterial and abiotic oxidation of pyrite. Geochim. Cosmochim. Acta (71), 3796.

Banfield, J.L., Moreau, J.W., Chan, C.S., Welch, S.A., Little, B., 2001. Mineralogical biosignatures and the search for life on Mars. Astrobiology (1), 447.

Bao, H., Thiemens, M., 2000a. Generation of O2 from BaSO4 using a CO2 laser fluorination system for simultaneous analysis of δ18O and δ17O. Anal. Chem. 72, 4029–4032.

Bao, H., Lyons, J.R., Zhou, C., 2008. Triple oxygen isotope evidence for elevated CO2 levels after a neoproterozoic glaciation. Nature 453, 504.

Bao, H., Fairchild, I.J., Wynn, P.M., Spotl, C., 2009. Stretching the envelope of past surface environments: neoproterozoic glacial lakes from svalbard. Science 323, 119–122.

Bao, H., Cao, X., Hayles, J., 2015. The confines of triple oxygen isotope exponents in elemental and complex mass-dependent processes. Geochim. Cosmochim. Acta 170, 39–50.

Bao, Z., Bain, J., Saurette, E., Finfrock, Y.Z., Hu, Y., Ptacek, C.J., Blowes, D.W., 2022. Mineralogy-dependent sulfide oxidation *via* polysulfide and thiosulfate pathways during weathering of mixed-sulfide bearing mine waste rock. Geochim. Cosmochim. Acta 317, 523–537.

Betts, R.H., Voss, R.H., 1970. The kinetics of oxygen exchange between the sulfite ion and water. Can. J. Chem. 48, 2035.

Brunner, B., Bernasconi, S.M., Kleikemper, J., Schroth, M., 2005. A model for oxygen and sulfur isotope fractionation in sulfate during bacterial sulfate reduction processes. Geochim. Cosmochim. Acta 69, 4773–4785.

Brunner, B., Yu, J.-Y., Mielke, R.E., MacAskill, J.A., Madzunkov, S., McGenity, T.J., Coleman, M.L., 2008. Different isotope and chemical patters related to lag and exponential growth phases of *acidithiobacillus ferrooxidans* reveal a microbial growth strategy. Earth Planet. Sci. Lett. 270, 63.

Cao, X., Bao, H., 2021. Small triple oxygen isotope variations in sulfate: mechanisms and applications. Rev. Mineral. Geochem. 86, 463–488.

Chiba, H., Sakai, H., 1985. Oxygen isotope exchange rate between dissolved sulfate and water at hydrothermal temperatures. Geochim. Cosmochim. Acta 49, 993.

Cowie, B.R., Johnston, D.T., 2016. High-precision measurement and standard calibration of triple oxygen isotopic compositions (d18O, D17O) of sulfate by F2 laser fluorination. Chem. Geo. 440, 50–59.

Crockford, P.W., Cowie, B.R., Johnston, D.T., Hoffman, P.F., Sugiyama, I., Pellerin, A., Bui, T.H., Hayles, J., Halverson, G.P., Macdonald, F.A., Wing, B.A., 2016. Triple oxygen and multiple sulfur isotope constraints on the evolution of the post-marinoan sulfur cycle. Earth Planet. Sci. Lett. 435, 74–83.

Descostes, M., Vitorge, P., Beaucaire, C., 2004. Pyrite dissolution in acidic media. Geochim. Cosmochim. Acta 68, 4559.

Druschel, G., Borda, M., 2006. Comment on "pyrite dissolution in acidic media" by M. Descostes, P. Vitorge, and C. Beaucaire. Geochim. Cosmochim. Acta 70, 5246–5250.

Fernandez-Remolar, D., Gomez-Elvira, J., Gomez, E., Sebastian, F., Martiin, J., Manfredi, J.A., Torres, J., Gonzales Kessler, C., Amils, R., 2004. The Tinto River, an extreme acidic environment under control of iron, as an analogue of the *Terra Meridiani* hematite site of Mars. Planet. Space Sci. 52, 239.

Gleisner, M., Herbert Jr, R.B., Frogner Kockum, P.C., 2006. Pyrite oxidation by *acidithiobacillus ferrooxidans* at various concentrations of dissolved oxygen. Chem. Geol. 225, 16.

Gomes, M.L., Johnston, D.T., 2017. Oxygen and sulfur isotopes in sulfate in modern euxinic systems with implications for evaluating the extent of euxinia in ancient oceans. Geochim. Cosmochim. Acta 205, 331–359.

Halevy, I., Peters, S.E., Fischer, W.W., 2012. Sulfate burial constraints on the Phanerozoic sulfur cycle. Science 337, 6092.

Hayles, J.A., Cao, X., Bao, H., 2017. The statistical mechanical basis of the triple isotope fractionation relationship. Geochem. Perspect. Lett. 3, 1–11.

Heidel, C., Tichomirowa, M., 2011. The isotopic composition of sulfate from anearobic and low-oxygen pyrite oxidation experiments with ferric iron- new insights into oxidation mechanisms. Chem. Geol. 281, 305.

Heidel, C., Tichomirowa, M., Junghans, M., 2013. Oxygen and sulfur isotope investigations of the oxidation of sulfide mixtures containing pyrite, galena, and sphalerite. Chem. Geol. 342, 29–43.

Helman, Y., Barkan, E., Eisenstadt, D., Luz, B., Kaplan, A., 2005. Fractionation of three stable oxygen isotopes by oxygen-producing and oxygen-consuming reactions in photosynthetic organisms. Plant. Physiol. 138, 2292.

Hemingway, J.D., Olson, H., Turchyn, A.V., Johnson, D.T., 2020. Triple oxygen isotope insight into terrestrial pyrite oxidation. PNAS 117 (14), 7650–7657.

Horner, D.A., Connick, R.E., 2003. Kinetics of oxygen exchange between the two isomers of bisulfite ion, disulfite ion, and water as studied by oxygen-17 nuclear magnetic resonance spectroscopy. Inorg. Chem. 42, 1884–1894.

Hubbard, C.G., Black, S., Coleman, M.L., 2009. Aqueous geochemistry and oxygen isotope compositions of acid mine drainage from the Rio Tinto, SW SPain highlight inconsistencies in current models. Chem. Geol. 265, 321.

Jones, S., Santini, J.M., 2023. Mechanisms of bioleaching: iron and sulfur oxidation by acidophilic microorganisms. Essays Biochem. 67, 685–699.

Killingsworth, Bryan A., Bao, Huiming, Kohl, Issaku E., 2018. Assessing pyrite-derived sulfate in the Mississippi River with four years of sulfur and triple-oxygen iso-tope data. Environ. Sci. Technol. 52 (11), 6126–6136.

Killingsworth, B.A., Cartigny, P., Hayles, J.A., Thomazo, C., Sansjofre, P., Pasquier, V., Lalonde, S.V., Philippot, P., 2022. Towards a holistic sulfate-water-O2 triple oxygen systematics. Chem. Geol. 588, 1–14.

Kim, D-M., Yun, S.-T., Yoon, S., Mayer, B., 2019. Signature of oxygen and sulfur isotopes of sulfate in ground and surface water reflecting enhanced sulfide oxidation in mine areas. Appl. Geochem. 100, 143–151.

Kohl, I., Bao, H., 2011. Triple-oxygen isotope determination of molecular oxygen incorporation in sulfate produced during abiotic oxidation of pyrite (pH=2-10). Geoch. et Chosmochim. Acta 75, 1785.

Krouse, H.R., Gould, W.D., McCready, R.G.L., Rajan, S., 1991. 18O incorporation into sulfate during the bacterial oxidation of sulfide minerals and the potential for oxygen isotope exchange between O2, H2O and oxidized sulfur intermediates. Earth Planet Sci. Lett. 107, 90–94.

Mielke, R.E., Pace, D.L., Porter, T., Southam, G., 2003. A critical stage in the formation of acid mine drainage: colonization of pyrite by *acidithiobacillus ferrooxidans* under pH-neutral conditions. Geobiology 1, 81–90.

Moses, C.O., Nordstrom, D.K., Herman, J.S., Mills, A.L., 1987. Aqueous pyrite oxidation by dissolved oxygen and by ferric iron. Geochim. Cosmochim. Acta 51, 1561–1571.

Müller, I.A., Brunner, B., Coleman, M.L., 2013. Isotopic evidence of the pivotal role of sulfite exchange in shaping the oxygen isotope signature of sulfate. Chem. Geol. 354, 186.

Pack, A., Tanaka, R., Hering, M., Sengupta, S., Peters, S., Nakamura, E., 2016. The oxygen isotope composition of San Carlos Olivine on the VSMOW2-SLAP2 scale. Rapid Commun. Mass Spectrom. 30, 1495.

Pisapia, C., Chaussidon, M., Mustin, C., Humbert, B., 2007. O and S isotopic compositions of dissolved and attached oxidation products of pyrite oxidation by *acidithiobacillus ferrooxidans*: comparison with abiotic oxidations. Geochim. Cosmochim. Acta 71, 2474.

Reedy, B.J., Beattie, J.K., Lowson, R.T., 1991. A vibrational spectroscopic 18O tracer study of pyrite oxidation. Geochim. Cosmochim. Acta 55, 1609–1614.

Rennie, Victoria C.F., Turchyn, Alexandra V., 2014. Controls on the abiotic ex-change between aqueous sulfate and water under laboratory conditions. Limnol. Oceanogr. Methods 12, 166–173.

Rimstidt, J.D., Vaughan, D.J., 2003. Pyrite oxidation: a state-of-the-art assessment of the reaction mechanism. Geochim. Cosmochim. Acta. 67, 873–880.

Rimstidt, D.J., Vaughan, D.J., 2014. Acid mine drainage. Elements 153–154.

Sharp, Z.D., Wostbrock, J.A.G., 2021. Standardization for the triple oxygen isotope system: waters, silicates, carbonates, air, and sulfates. Rev. Min. Geochem. 86, 179–196.

Sharp, Z.D., Wostbrock, J.A.G., Pack, A., 2018. Mass-dependent triple oxygen isotope variations in terrestrial materials. Geochem. Persp. Let. 7, 27–31.

Singer, P.C., Stumm, W., 1970. Acid mine drainage: the rate-determining step. *Sci.* New Series 167, 1121.

Taylor, B.E., Wheeler, M.C., Nordstrom, D.K., 1984. Stable isotope geochemistry of acid mine drainage: experimental oxidation of pyrite. Geochim. Cosmochim. Acta 48, 2669.

Taylor, B.E., Wheeler, M.C., 1994. Sulfur-and oxygen-isotope geochemistry of acid mine drainage in the western United States: field and experimental studies revisited. Environmental Geochemistry of Sulfide Oxidation, pp. 481–514.

Tichomirowa, M., Junghans, M., 2009. Oxygen isotope evidence for sorption of molecular oxygen to pyrite surface sites and incorporation into sulfate in oxidation experiments. Appl. Geochem. 24 (11), 2072–2092.

Usher, C.R., Cleveland, Strongin, D.R., Schoonen, M.A., 2004. Origin of oxygen in sulfate during pyrite oxidation with water and dissolved oxygen: an in situ horizontal attenuated total reflectance spectroscopy isotope study. Eviron. Sci Technol. 38, 5604–5606.

Van Stempvoort, D.R., Krouse, H.R., 1994. Controls of δ18O in sulfate: Review of Experimental Data and Application to Specific Environments. ACS Publications.

Vera, M., Schippers, A., Hedrich, S., Sand, W., 2022. Progress in bioleaching: fundamentals and mechanisms of microbial metal sulfide oxidation - part A. Appl. Microbiol. Biotechnol. 106, 6933–6952.

Waldeck, A.R., Cowie, B.R., Bertran, E., Wing, B.A., Halevy, I., Johnson, D.T., 2019. Deciphering the atmospheric signal in marine sulfate oxygen isotope composition. Earth Planet. Sci. Lett. 522, 12–19.

Waldeck, A.R., Hemingway, J.D., Yao, W., Paytan, A., Johnston, D.T., 2022. The triple oxygen isotope composition of marine sulfate and 130 million years of microbial control. PNAS 119 (31). Epub Mar 25.

Wei, Y., Yan, H., Peng, Y., Bao, H., 2024. Quantitative conversions of sulfate oxygen for high-precision oxygen isotope analysis. Anal. Chem. 96, 19387–19395, 2024.

Williamson, M.A., Rimstidt, J.D., 1994. The kinetics and rate determining step of aqueous pyrite oxidation. Geochim. Cosmochim. Acta 58, 5443.

Young, E.D., Galy, A., Nagahara, H., 2002. Kinetic and equilibrium mass-dependent fractionation laws in nature and their geochemical and cosmochemical significance. Geochim. Cosmochim. Acta 66, 1095.

Young, E.D., Yeung, L.Y., Kohl, I.E., 2014. On the Δ17O budget of atmospheric O2. Geochim. Cosmochim. Acta 135, 120.

Yu, J.-Y., McGenity, T.J., Coleman, M.L., 2001. Solution chemistry during the lag phase and exponential phase of pyrite oxidation by *thiobacillus ferrooxidans*. Chem. Geol. 175, 307.